Supporting Information

Giant Electric Field Dependent Hole Mobility of $CsPbBr_3$ Nanocrystals Films

Shipei Sun[a], Hui Bao[a], Lihao Liu[a], Jiahao Wan[a], Haitao Wang[a], Yunan Gao[b,*] and Haizheng Zhong[a,*]

[a] MIIT Key Laboratory for Low Dimensional Quantum Structure and Devices, School of Materials Science and Engineering, Beijing Institute of Technology, 100081 Beijing, China.

[b] Key Laboratory of Luminescence and Optical Information, Ministry of Education, School of Physical Science and Engineering, Beijing Jiaotong University, Beijing, P. R. China

Corresponding Authors:

HaiZheng Zhong. (hzzhong@bit.edu.cn).

Yunan Gao. (gyn@pku.edu.cn).

Part 1 Experiment and measurements

Materials

N-hexane, chlorobenzene1-octadecene (ODE, 90%), oleic acid (OA, 90%), oleylamine (OLA, 90%), lead(II) oxide (PbO, 99.9%), n-tetradecylamine (TDA, 90%), Didodecyldimethylammonium bromide (DDAB, 99%), cesium carbonate (Cs_2CO_3, 99%), Molybdenum trioxide (MoO_3) bromobenzaldehyde (C_7H_5BrO), were purchased from Aladdin, China. (LiF, 99.85%, Alfa Aesar), Poly(3,4-ethylenedioxythiophene):poly(styrene sulfonate) (PEDOT: PSS), poly [(9,9-dioctylfluorenyl-2,7-diyl)-alt-(4,4′-(N-(4-butylphenyl) (TFB), 1,3,5-tris(1-phenyl-1H-benzimidazol-2-yl) benzene (TPBI) were purchased from Xi'an Polymer Light Technology Corp.

Synthesis of $CsPbBr_3$ nanocrystal.

This method is based on the previous report by the author.[1] A mixture of 18 mL ODE, 2 mL OA, 0.46 g Cs_2CO_3 was degassed with vacuum (140 ℃, 1 hour). And 0.046 g PbO, 0.120 g C_7H_5BrO, 1 mL OA and 10 mL of ODE were added to the flask and heated to 220 ℃. Subsequently, 0.3 mL OLA was injected at 120-250℃ to obtain different size $CsPbBr_3$ (for 15 minutes continuously). Then, 0.5 mL of precursor was rapidly injected into the flasks, and the reaction mixture was cooled rapidly by ice bath. The resulting solution was centrifuged twice at 6000 rpm and then added with hexane to obtain the twelve-faced $CsPbBr_3$ nanocrystals (NCs).

Single hole-carrier device fabrication.

The ITO-coated glass substrates were cleaned sequentially using detergent, acetone, and isopropanol in an ultrasonic bath for 30 min each. After cleaning, they were treated with ozone plasma for 5 min. Next, a PEDOT:PSS solution was spin-coated onto the ITO substrates at 6,000 rpm for 60 s and then annealed at 150 °C for 15 min. The coated substrates were then transferred into a nitrogen-filled glovebox for the deposition of subsequent layers. The TFB layer was spin-coated at 2,000 rpm for 30 s from an 10 mg ml^{-1} chlorobenzene solution, followed by baking at 150 °C for 30 min. Next, the QD layer (20 mg ml^{-1}) was spin-coated at 2,000 rpm for 30 s, followed by baking at 80 °C for 5 min. MoO_3 (5 nm) and Al (80 nm) were deposited by thermal evaporation under vacuum of about 2.0×10^{-4} Pa. The structure of hole-carrier device is ITO/PEDOT:PSS/ TFB/QDs/MoO_3/Al (device A).

Part 2 Monte Carlo Simulation and Wentzel-Kramers-Brillouin

2.1 Monte Carlo Simulation

This study uses a three-dimensional Miller-Abrahams method to simulate the hopping transport

process of carriers in $CsPbBr_3$ NCs films. The simulated system consists of a bottom electrode, an active layer, and a top electrode, with overall dimensions of $L_x \times L_y \times L_z$, where the *xyz* values are adjustable ($L_x = L_y = 200\ nm$, $L_z = 320\ nm$). The nanocrystal array is arranged in a simple cubic (SC) or face-centered cubic (FCC) lattice, with anisotropic spacing set as $\Delta x = \Delta y = \Delta z$, satisfying the physical constraints $\Delta x > 2R$, $\Delta y > 2R$, $\Delta z > 2R$ (R is the radius of the $CsPbBr_3$ NCs). The electrode region has a thickness d = 10 nm, located at the top and bottom surfaces of the film. The energy of the $CsPbBr_3$ NCs in the active layer follows a Gaussian distribution $\varepsilon_i \sim N(0, \sigma^2)$, where the energetic disorder σ is calculated using a size-correction formula:

$$\sigma = \sigma_{\text{base}} \cdot \frac{R_{\text{base}}}{R}$$

Here, $\sigma_{base}\ is\ 0.05$ eV. Carrier transport follows the hopping model, and the hopping rate from position *i* to *j* is given by:[2]

$$r_{ij} = \nu_0 exp(-\frac{2r_{ij}}{\xi}) \cdot \Gamma(\Delta E_{ij})$$

Here, ν_0 is attempt frequency (10^{12} Hz), r_{ij} is distance of nanocrystals, the effective energy difference ΔE_{ij} includes both the energy difference and the contribution from the applied electric field:[3]

$$\Delta E_{ij} = (\varepsilon_j - \varepsilon_i) + V \cdot \frac{z_j - z_i}{L_z}$$

Heat accessory factor $\Gamma(\Delta E)$:

$$\Gamma(\Delta E) = \begin{cases} 1 & \Delta E \le 0 \\ \exp\left(-\frac{\Delta E}{k_B T}\right) & \Delta E > 0 \end{cases}$$

Here, V is applied voltage, T is 300 K.

The simulation starts from the center of the bottom electrode, searching for nearby quantum dots within a radius of $4 \cdot max(\Delta x, \Delta y, \Delta z)$. Each hopping process consists of three steps: (1) Calculate the hopping rates r_{ij} for all neighbors and the total rate $R_{total} = \sum r_{ij}$; (2) Randomly select a target site according to the probability r_{ij}/R_{total}; (3) Calculate the hopping time $\Delta t = -ln(U)/R_{total}$ (U is a uniformly distributed random number between 0 and 1). The simulation termination conditions include: (a) the electron reaches the top electrode; (b) the total rate falls below 10^{-30} s^{-1}; (c) the number of hops exceeds the threshold $N_{max} = 10000$. The transmission path is visualized through a 3D trajectory, with the trajectory color mapping time evolution information.

This model quantitatively reveals the synergistic mechanism of inter-dot spacing, energy disorder, and temperature under electric field regulation, providing a theoretical tool for the optimization of perovskite optoelectronic devices.

2.2 WKB tunneling:

The WKB approximation, as a semiclassical method for dealing with one-dimensional barrier tunneling problems, has a core model expression in the exponential form of the tunneling probability. A research method for carrier dynamics in quantum dot devices based on the Wentzel-Kramers-Brillouin (WKB) tunneling model. This model provides a quantitative analysis of carrier transport in nanocrystals.[4]

$$T \approx exp(-\frac{2}{\hbar}\int_{x_1}^{x_2} \sqrt{2m^*(V(x) - E)}dx)$$

Here, E(x) is barrier potential height, m^* denotes the carrier effective mass, x_1 and x_2 denote the start and end points of the barrier, respectively and $\hbar$ the reduced Planck constant. Eq.1 indicates the relationship of the tunneling efficiency (Γ) and energy barrier. This expression reveals the intrinsic characteristic of the tunneling probability exponentially decaying with barrier parameters, as well as the coupling relationship between effective mass and barrier parameters.

Part 3 Tables.

Table S1 Average hole mobility of $CsPbBr_3$ NCs.

Size (nm)	Hole mobility (cm^2/Vs) ($\times10^{-9}$)			Average mobility (cm^2/Vs) ($\times10^{-9}$)	Standard Deviation
9	0.38	0.43	0.37	0.39	0.43
12	0.78	0.81	0.78	0.78	0.81
14.5	0.92	0.95	0.9	0.93	0.95
17	1.03	1.0	1.08	1.03	1.0
22	1.84	1.80	1.89	1.85	1.80
26	2.61	2.51	2.55	2.62	2.51

Table S2 The comparison of $CsPbBr_3$ QD mobility data measured in other articles.

Materials	ligand	Carrier Mobility ($m^2\ V^{-1}\ s^{-1}$)	Method	References
$CsPbBr_3$ QD (26 nm)	OA/OLA (18C)	μe 5.4×10^{-13}–4.36×10^{-12} μh 3.9×10^{-13}–4.0×10^{-11}	SCLC	This work
$CsPbBr_3$ QD	OA	μ_e 8.14×10^{-11}	SCLC	Adv. Optical Mater. 2025, 13, 2403039
$CsPbBr_3$ QD	Butylamine（4C）	μ_h 7×10^{-11}	FET	ACS Energy Lett. 2019, 4, 534−541
$CsPbAgBr_3$ QD	Butylamine（4C）	μ_h 8×10^{-8}	FET	ACS Energy Lett. 2019, 4, 534−541
$CsPbBr_3$ QD	oleyl amine /oleic acid (18C)	μ_h 6.5×10^{-14}	SCLC	Adv. Optical Mater. 2025, 13, e01361
$CsPbBr_3$ QD	DDAB (12C)	μ_e 1.5×10^{-10}	SCLC	Adv. Optical Mater. 2025, 13, e01361
Unspecified QDs	/	$\mu_{h\text{-}e}$ 1×10^{-7} –1×10^{-10}	Numerical simulation	J. Appl. Phys. 126, 035704 (2019)
$CsPbBr_3$ QD	OA/OLA (18C)	μ_e 2.1×10^{-4} μ_h 6.9×10^{-3}	Monte Carlo simulation	ACS Appl. Mater. Interfaces 2021, 13, 44742−44750
$CsPbBr_3$ QD	Mercaptopropionic acid (3C)	μ_e 5×10^{-7}	SCLC	Nanomaterials 2020, 10, 1297;
$CsPbBr_3$ QD	IPABr/NaBr (1C)	$\mu_{e\text{-}h}$ 1×10^{-6}	SCLC	Nature Nanotechnology volume 15, pages668–674 (2020)
Materials	**ligand**	**Carrier Mobility ($m^2\ V^{-1}\ s^{-1}$)**	**Method**	**References**
$CsPbBr_3$ QD	OA/OLA (18C)	μ_h 6.1×10^{-9}	SCLC	J. Mater. Chem. C, 2021, 9, 11324–11330
$CsGaPbBr_3$ QD	OA/OLA (18C)	μ_h 3.6×10^{-8}	SCLC	J. Mater. Chem. C, 2021, 9, 11324–11330

$CsPbBr_3$ QD	THPABr (4C+Benzene)	μ_h 4.79 × 10^{-8} μ_e 4.34 × 10^{-9}	SCLC	Chemical Engineering Journal 501 (2024) 157596
$CsPbBr_3$ QD	PPABr (4C+Benzene)	μ_h 6.94 × 10^{-8} μ_e 7.32 × 10^{-9}	SCLC	Chemical Engineering Journal 501 (2024) 157596
$CsPbBr_3$ QD	4-CH_3-PPABr (5C+Benzene)	μ_h 9.36 × 10^{-8} μ_e 6.82 × 10^{-9}	SCLC	Chemical Engineering Journal 501 (2024) 157596
$CsPbBr_3$ QD	4-F-PPABr (5C+Benzene)	μ_h 6.9 × 10^{-8} μ_e 8.4 × 10^{-9}	SCLC	Chemical Engineering Journal 501 (2024) 157596
$CsPbBr_3$ QD	PEABr/MBABr (3C+Benzene)	μ_h 3.5 × 10^{-7}	SCLC	Nature volume 612, pages679–684 (2022)

Table S3 Total time and jumps for 10000 Monte Carlo Simulation runs.

Size (nm)	Total Time (s)	Jumps
8	3.07×10^{-11}	95
10	8.34×10^{-12}	32
12	6.20×10^{-12}	25
14	5.47×10^{-12}	22
16	5.41×10^{-12}	21
18	4.71×10^{-12}	20
20	4.19×10^{-12}	17
22	4.09×10^{-12}	16
24	3.69×10^{-12}	14
26	3.33×10^{-12}	15
30	2.76×10^{-12}	11

Part 4 Pictures.

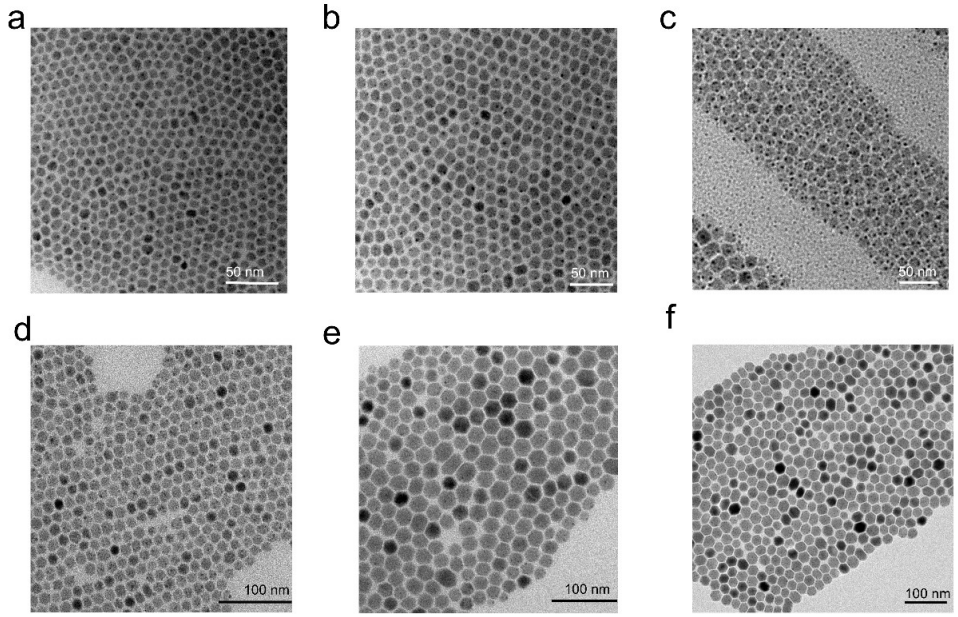

Figure S1 TEM image of $CsPbBr_3$ NCs. (a) 9 nm. (b) 12 nm. (c) 14.5 nm. (d) 17 nm. (e) 22 nm. (f) 26 nm.

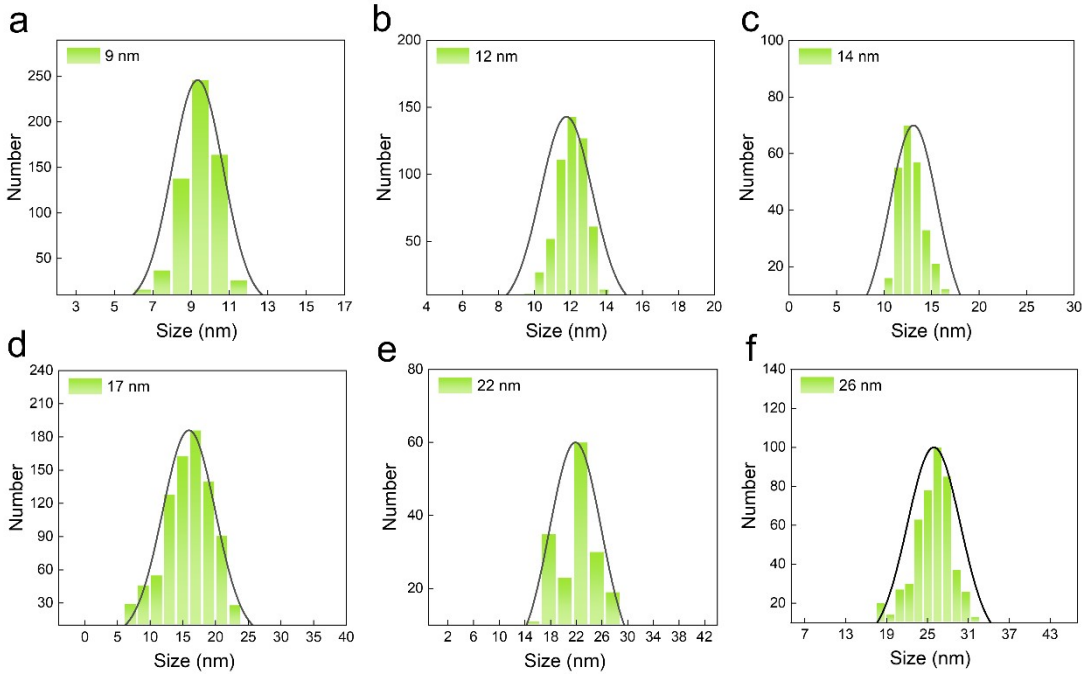

Figure S2 The histogram of different $CsPbBr_3$ NCs size. (a) 9 nm. (b) 12 nm. (c) 14.5 nm. (d) 17 nm. (e) 22 nm. (f) 26 nm.

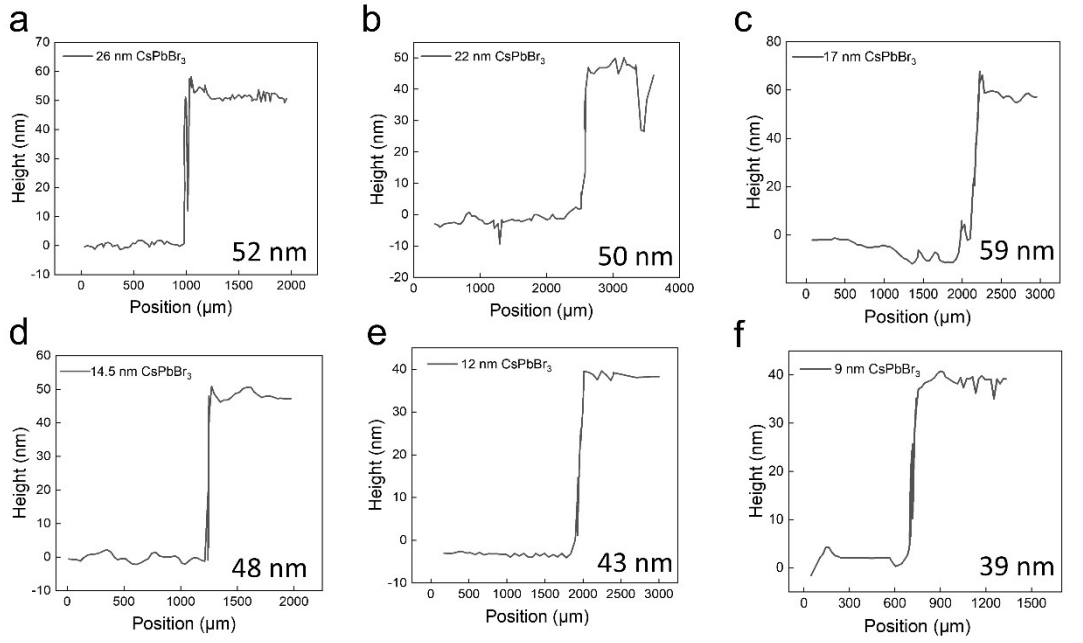

Figure S3 The thickness of different $CsPbBr_3$ NCs size. (a)52 nm. (b) 50 nm. (c) 59 nm. (d) 48 nm. (e) 43 nm. (f) 39 nm.

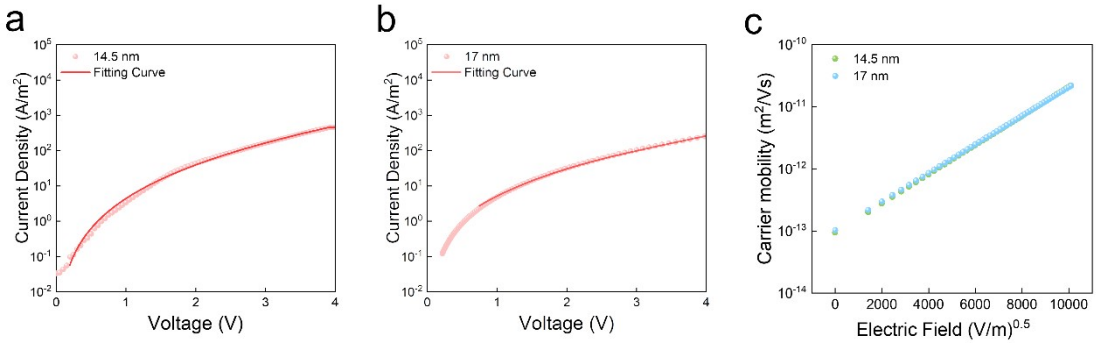

Figure S4 (a) The hole-only J-V curves of $CsPbBr_3$ NCs with 14.5 nm and corresponding fitting using NS-SCLC. (b) The hole-only J-V curves of $CsPbBr_3$ NCs with 14.5 nm and corresponding fitting using NS-SCLC. (c) The electric field dependent carrier mobility of different size $CsPbBr_3$ NCs.

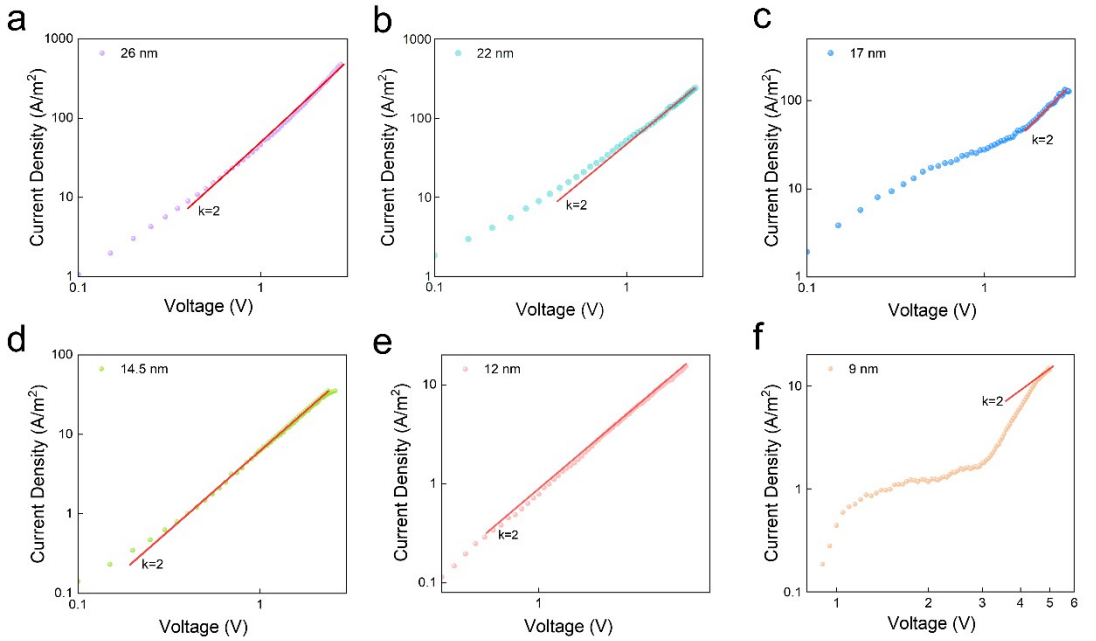

Figure S5 The electron-only J-V curves of $CsPbBr_3$ NCs and corresponding fitting using NS-SCLC. (a) 26 nm. (b) 22 nm. (c) 17 nm. (d) 14.5 nm. (e) 12 nm. (f) 9 nm.

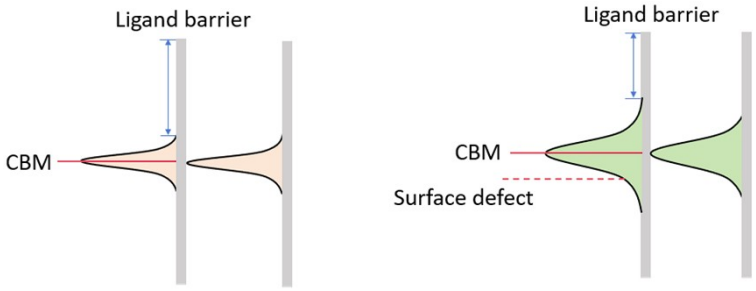

Figure S6 Charge transport processes in CsPbBr3 NCs.

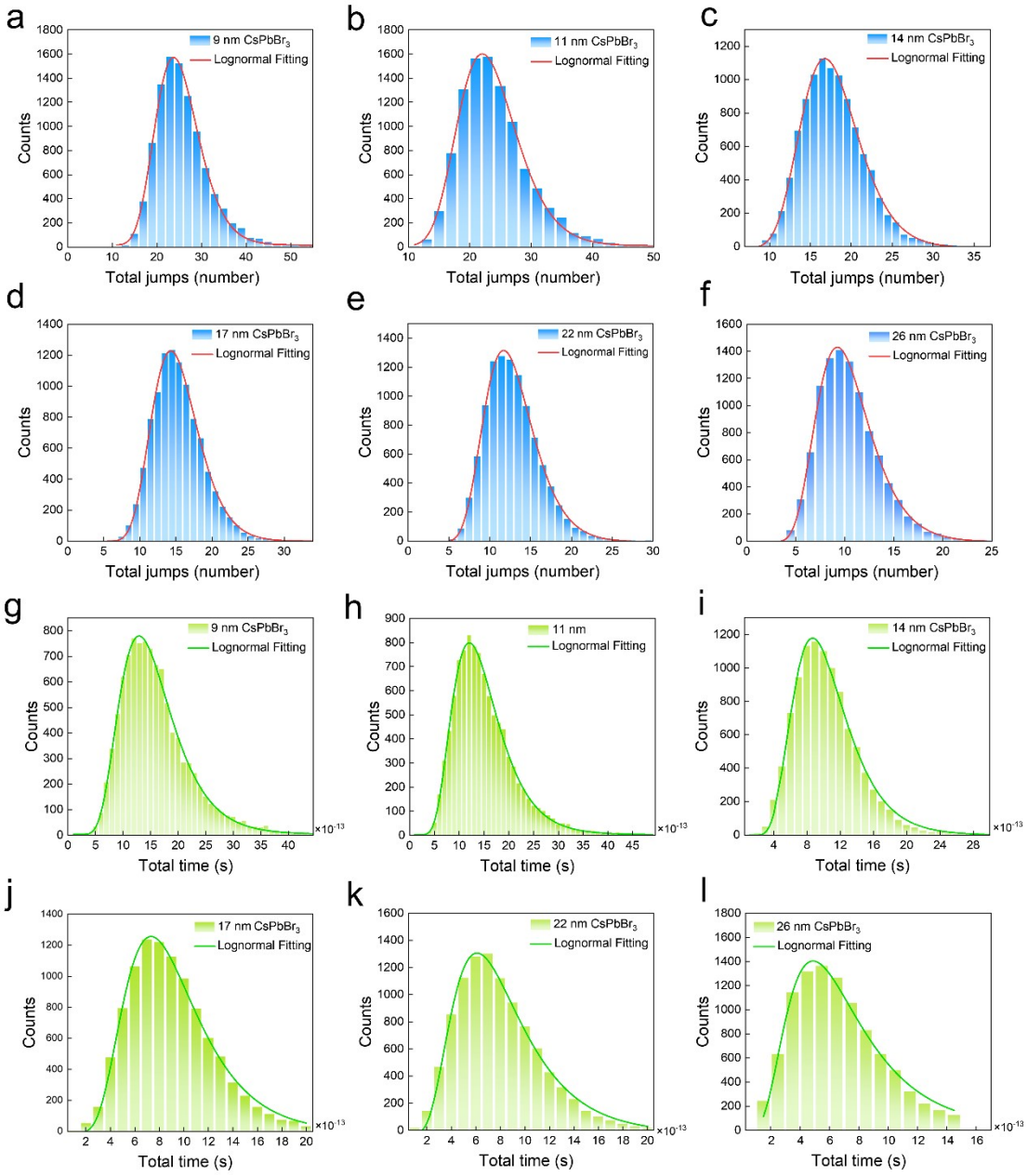

Figure S7 These data are the results of averaging 10000 simulation runs.

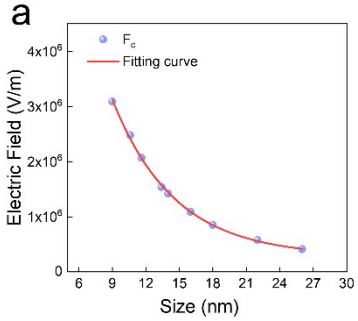

Figure S8 Applying an electric field is necessary to overcome charging energy effects in different size $CsPbBr_3$ NCs.

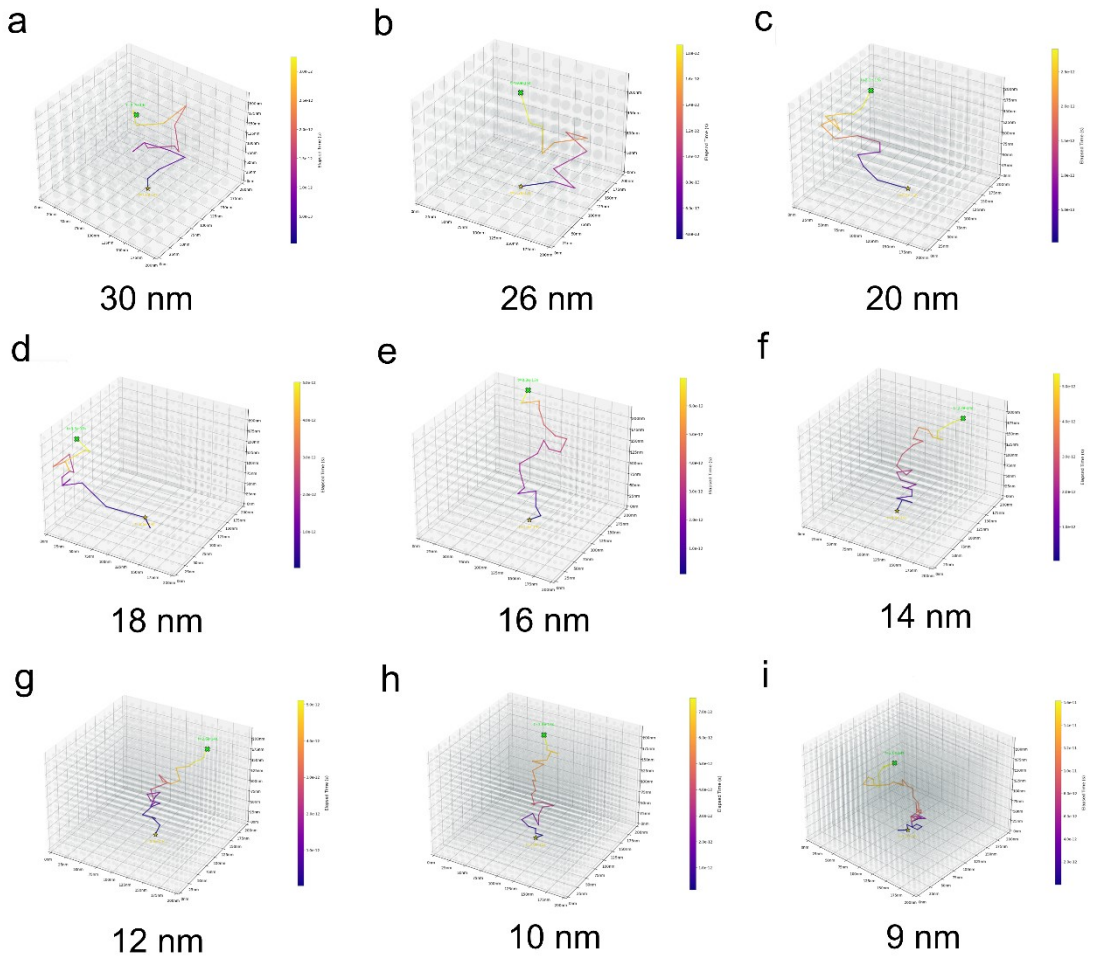

Figure S9 Carrier trajectories under 20 V for 50 Monte Carlo simulations. (a) 30 nm. (b) 26 nm. (c) 20 nm. (d) 18 nm. (e) 16 nm. (f) 14 nm. (g) 12 nm. (h) 10nm. (i) 9 nm.

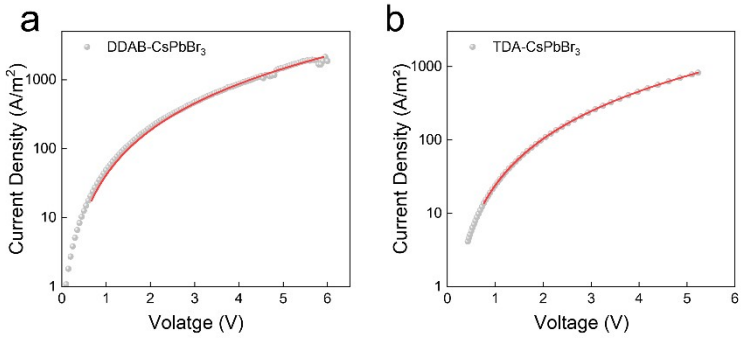

Figure S10 (a) The J-V curves of $CsPbBr_3$ NCs with DDAB ligand and corresponding fitting using NS-SCLC. (b) The J-V curves of $CsPbBr_3$ NCs with TDA ligand and corresponding fitting using NS-SCLC.

Reference

1. S. Sun, P. Huang, X.-g. Wu, C. Chen, X. Hu, Z. Bai, A. Pushkarev and H. Zhong, *J. Phys. Chem. C.*, 2024, **128**, 3602-3608.
2. Y. Xing, N. Yazdani, W. M. M. Lin, M. Yarema, R. Zahn and V. Wood, *ACS Appl. Electron. Mater.*, 2022, **4**, 631-642.
3. C. Data Handling Division, Geneva, Switzerland, *Rep. Prog. Phys.*, 1980, **43**.
4. Z. H. Huang, T. E. Feuchtwang, P. H. Cutler and E. Kazes, *Phys. Rev. A*, 1990, **41**, 32-41.